Available online at www.sciencedirect.com

ScienceDirect

journal homepage: www.elsevier.com/locate/he

CO selective oxidation using Co-promoted Pt/γ-Al_2O_3 catalysts

Natalia E. Nuñez [a,b], Hernán P. Bideberripe [a,b], Martín Mizrahi [c], José Martín Ramallo-López [c], Mónica L. Casella [a], Guillermo J. Siri [a,b,*]

[a] Centro de Investigación y Desarrollo en Ciencias Aplicadas "Dr. Jorge Ronco" (CINDECA), Facultad de Ciencias Exactas, UNLP – CCT La Plata – CONICET, Calle 47 N°257, 1900 La Plata, Argentina

[b] PIDCAT, Facultad de Ingeniería, Universidad Nacional de La Plata UNLP, Calle 1 esq. 47, 1900 La Plata, Argentina

[c] Instituto de Investigaciones Fisicoquímicas Teóricas y Aplicadas (INIFTA) (CCT La Plata-CONICET, UNLP) Facultad de Ciencias Exactas, Universidad Nacional de la Plata, Diagonal 113 y calle 64, P.O.Box 16 Suc. 4, 1900 La Plata, Argentina

ARTICLE INFO

Article history:
Received 24 August 2015
Received in revised form
24 August 2016
Accepted 26 August 2016
Available online 22 September 2016

Keywords:
Hydrogen purification
PEM fuel cell
Preferential CO oxidation
$PtCo/Al_2O_3$
EXAFS–XANES

ABSTRACT

In this work, alumina-supported platinum catalysts promoted with cobalt were analyzed in the preferential CO oxidation (PROX) reaction. The addition of Co represents a significant catalytic improvement with regard to the monometallic Pt catalyst. This improvement reaches its maximum with a Co/Pt atomic ratio of 1.5. The addition of a higher level of cobalt decreases the activity probably because it would produce the coverage of the Pt active sites, thus inhibiting the adsorption of CO. For all the bimetallic catalysts, the maximum conversion occurs at *ca.* 130 °C, a value which is within the acceptable working range for this process. A further temperature increase generates a decrease in the CO conversion. The studied catalysts presented a slight deactivation after several hours on stream. The original activity is recovered by submitting the catalysts to a reduction process at 500 °C. Results are explained in terms of TPR, DRS, EXAFS and XANES characterization of the catalysts.

Introduction

A variety of fuel cells have been developed having a wide field of application. For power generation both in mobile and stationary sources, proton exchange membrane fuel cells (PEMFC) appear as the most important. These cells produce electricity through an electrochemical reaction, so that their efficiency is not limited by the Carnot cycle. The anode of the cell is made of platinum, using hydrogen as fuel. They have advantages such as high efficiency, low operating temperature, quick start and mainly, they do not emit pollutants to the environment [1]. However, these same advantages are diminished when considering the fuel supply: pure hydrogen presents problems with its carriage and storage [2], besides, it has low energy per unit volume compared to other gaseous fuels and a high power is required to achieve its compression. A feasible alternative is to produce *in situ* the hydrogen to feed the cells.

* Corresponding author. Centro de Investigación y Desarrollo en Ciencias Aplicadas "Dr. Jorge Ronco" (CINDECA), Facultad de Ciencias Exactas, UNLP – CCT La Plata – CONICET, Calle 47 N°257, 1900 La Plata, Argentina
E-mail addresses: gsiri@quimica.unlp.edu.ar, siri.guillermo@gmail.com (G.J. Siri).

http://dx.doi.org/10.1016/j.ijhydene.2016.08.170
0360-3199/

Hydrogen can be generated through different processes: reforming, Water Gas Shift Reaction (WGSR), Kvaerner Process, coal gasification and fermentation of organic compounds. The most widely used method of production of hydrogen is the reforming, which generates a gas mixture (syngas) composed of variable amounts of carbon monoxide and hydrogen. The CO present in this stream must be eliminated because, when it is fed together with hydrogen to the fuel cell, is preferentially adsorbed on the platinum anode preventing the hydrogen oxidation reaction to occur [3]. According to current standards, the maximum amount of CO present in the feeding of PEMFC should be between 10 and 100 ppm [4]. The reforming of natural gas, methanol or gasoline generates a gas stream containing between 5 and 9% of CO [5]. After the reforming process, the gas mixture obtained is submitted to a two-steps WGSR: a first step at high temperature (HTS) between 350 and 600 °C, and a second step at low temperature (LTS), from 150 to 300 °C [6]. This reaction (Eq. (1)) allows to further reduce the content of CO to values between 0.2 and 2%.

$$CO + H_2O \leftrightarrow CO_2 + H_2 \quad \Delta H_{298} = \frac{kJ}{mol} \tag{1}$$

The WGSR is effective for the conversion of CO to CO_2, but because of its moderate exothermicity, is thermodynamically unfavorable at high temperature. An increase in temperature causes the conversion of CO to decrease [6].

There are several methods to further reduce the content of CO in H_2-rich streams and achieve a mixture that could be fed to a PEM fuel cell, including: catalytic methanation of CO, selective diffusion using Pd membranes, cryogenic methods, adsorption through pressure changes and PROX. Selective diffusion, methanation and PROX are the most promising methods [4]. The preferential oxidation has as main advantage its low cost and simple implementation without involving significant loss of hydrogen [7].

The PROX reaction is a gas phase catalytic reaction through which CO is transformed into CO_2, a product that does not interfere with the normal operation of the PEMFC. The PROX reaction is represented by Eq. (2):

$$CO + \tfrac{1}{2}O_2 \leftrightarrow CO_2 \tag{2}$$

At the same time, the oxidation of hydrogen (Eq. (3)) must be avoided:

$$H_2 + \tfrac{1}{2}O_2 \leftrightarrow H_2O \tag{3}$$

At high temperatures undesired reactions may occur: Reverse Water Gas Shift Reaction and CO methanation. These reactions should be avoided because they consume one and three moles of H_2 per mole of CO, respectively, representing a significant loss of H_2 (Eqs. (4) and (5)) [3]:

$$CO_2 + H_2 \leftrightarrow CO + H_2O \tag{4}$$

$$CO + 3H_2 \leftrightarrow CH_4 + 2H_2O \tag{5}$$

The main requirements to be fulfilled by the catalysts used in the PROX reaction are: high activity at low temperature, achieving conversions higher than 99%, high selectivity to the CO oxidation reaction and high resistance to deactivation caused by the presence of CO_2 and H_2O in the feed stream. Besides, the high activity should be obtained at temperatures between the operating temperature of the low temperature WGSR (150°C-300 °C) and that of the PEMFC (80°C-100 °C) [7,8].

In the early 1960, the U.S. Company Engelhard Corporation, now belonging to BASF, developed and commercialized the first catalyst for the removal of CO used in the ammonia synthesis. This catalyst was supported on alumina and contained between 0.1 and 0.3 wt.% of platinum [9]. Currently, the catalysts used for the PROX reaction can be separated into three groups: gold-based catalysts, those containing other precious noble metals and those based on transition metal oxides. Although Au catalysts show higher activity and selectivity than Pt catalysts, especially in the low temperature range, they suffer deactivation due to sintering during PROX reaction. Another drawback of gold catalysts is that at high water content, the CO oxidation reaction is inhibited. Concerning transition metal oxide catalysts, their catalytic activity is usually superior to that of the noble metal catalysts at low temperature, but is necessary to improve their stability in the presence of H_2O [3].

Platinum containing catalysts are the systems which have been more extensively studied. In 1963, Cohn proposed that alumina-supported Pt catalysts were an effective system for the conversion of CO in excess hydrogen. According to literature, this catalyst exhibited its maximum conversion at temperatures close to 200 °C, with oxygen concentrations just above the value given by the stoichiometry of the reaction and without formation of methane. Zeolitic Pt catalysts showed that they were able to oxidize CO more selectively than alumina-supported platinum catalyst, but it was necessary to add an excess of O_2, with values of λ near 2, λ being the oxygen excess factor. In the presence of H_2O and CO_2, the following series of activity is observed for the selective oxidation of CO with Pt catalysts: Zeolite A > Mordenite > Zeolite X > γ Al_2O_3. The most interesting catalytic systems for the PROX reaction are those that combine the noble metal with some easily reducible second metal [10]. When metal promoters are added to the Pt/Al_2O_3 catalyst (either as a second metal or as an oxide), a significant increase is observed in the conversion of CO to CO_2. Among the promoters that have been used to improve the activity of platinum-supported catalysts it can be mentioned the following: alkali metals, iron, manganese, nickel, niobium and cobalt. In our research group, Sn and Ge-modified bimetallic catalysts have been prepared through surface-controlled reactions and revealed higher catalytic activity compared to the conventional monometallic Pt catalysts [11,12].

Among transition metals, cobalt has been described as the most effective promoter for the PROX reaction. In that sense, cobalt-modified platinum catalysts have shown good activity in this reaction due to the synergistic effect between cobalt and platinum.

In this investigation, it was studied the preferential CO oxidation in excess H_2 over alumina-supported Co modified Pt catalytic systems. We examined the influence of the Co/Pt ratio on the catalytic performance, in order to find a catalyst that achieved a CO concentration in the outlet gas that were within the acceptable limits for feeding a PEMFC. In addition, a detailed characterization of the catalysts was carried out.

Besides, in the present paper, we also report on the stability of the catalysts, demonstrating that they present a more than acceptable CO conversion in a realistic condition over a considerable period of time.

Experimental section

Catalyst preparation

A commercial γ-Al_2O_3 (Air Products) with a pore volume of 0.63 cm^3/g and a surface area of 252 m^2/g, was used as support. The solid was crushed and sieved to obtain particles in the range 60–100 mesh and before being used, it was submitted to a calcination process in air at 500 °C for 4 h.

Platinum was added to the support by ion exchange using an aqueous solution of hexachloroplatinic acid (H_2PtCl_6, Sigma Aldrich) of concentration such as to provide the catalysts a Pt loading of 1wt. %. The solution and the support were left in contact for 24 h to enable the ionic exchange between them and then, the supernatant was removed and the solid was dried in oven for 3 h at 105 °C. Then, the catalyst was reduced at 500 °C for 2 h under a H_2 flow of 20 cm^3/min and subsequently it was repeatedly washed with aqueous ammonia until the complete removal of chloride. Finally, the solid was dried in an oven at 105 °C for 2 h. The monometallic catalyst so obtained is designated 1Pt.

The addition of cobalt to obtain the bimetallic catalysts was carried out by pore volume impregnation of the reduced monometallic catalysts (1Pt) with an aqueous solution of $Co(NO_3)_2 \cdot 6H_2O$ (Anedra, p.a.). After a contact time of 2 h, the preparation was dried in oven at 105 °C for 2 h. Table 1 lists all the bimetallic catalysts prepared and their metal loadings. It also indicates the atomic ratio between the two metals, which varied between 0 and 4. For some characterization tests, cobalt monometallic catalysts, with contents of 0.45 and 1.20 wt.% Co were also prepared.

Catalyst characterization

The analysis by atomic absorption spectrometry of the catalytic materials for platinum and cobalt determination was conducted in a Varian Spectra A 300 equipment. X-Ray Diffraction (XRD) patterns of the samples were recorded with a Philips PW 1050/70 diffractometer using CuKα radiation ($\lambda = 1.54$ Å) with a Ni filter, a current intensity of 20 mA and a high voltage supply of 40 kV. The diffractograms were recorded for a scanning angle (2θ) ranging from 5° to 70° at a scanning speed of 2.00°/min.

Temperature-Programmed Reduction (TPR) experiments were performed in laboratory constructed equipment. A 50 mg sample was placed in a 6 mm diameter quartz reactor. In a first step the sample was purged with Ar for 20 min at 20 °C to remove impurities and water contained in the catalyst. Then, the sample was heated from room temperature to 700 °C at a heating rate of 10 °C/min, while the reactor was fed at a flow rate of 10 cm^3/min of a reductive mixture composed of 5 vol.% H_2 in Ar. Hydrogen consumption was monitored using a Shimadzu GC-8A gas chromatograph equipped with a thermal conductivity detector (TCD).

The Diffuse Reflectance (DR) spectra of the calcined samples were recorded in the range 200–800 nm at room temperature, using a UV–vis spectrophotometer (Perkin Elmer LAMBDA 35) equipped with an integration sphere. The γ-Al_2O_3 support was used as a reference in all the cases and for dilution of the calcined samples. The powder samples were mounted in a quartz cell, which provided a sample thickness greater than 3 mm and thus guaranteed "infinite" sample thickness.

X-ray Absorption Spectroscopy (XAS) measurements were performed at the Laboratorio Nacional de Luz Synchrotron (Campinas, Brazil) using the XAFS2 beamline. The measurements were performed in the transmission mode using a Si(111) crystal monochromator in transmission mode and with three ion chambers as detectors. The third one was used to measure the corresponding metallic reference simultaneously with the sample. Samples were pressed to form a pellet and sealed in Ar atmosphere in special sample holders with kapton windows in order to avoid contact with air and were measured in that condition. The spectra were registered at room temperature at both the Pt L_3-edge (11.56 keV) and Co K-edge (7.71 keV). The EXAFS data were extracted from the measured absorption spectra by standard methods using the ATHENA software which is part of the IFFEFIT package [13]. The Fourier transformation was calculated using the Hanning filtering function. EXAFS modeling was carried out using the ARTEMIS program (IFFEFIT package). Structural parameters (coordination numbers and bond lengths and their mean squared disorders) were obtained by a nonlinear least-squares fit of the theoretical EXAFS signal to the data in R space by Fourier transforming both the theory and the data. Theoretical scattering path amplitudes and phase shifts for all paths used in the fits were calculated using the FEFF6 code [14].

Catalytic test (PROX)

The tests carried out to check the catalytic activity of each of the prepared catalysts were conducted in a glass reactor of 6 mm diameter, placed in an electric furnace at atmospheric pressure. A thermocouple was placed inside the reactor, which allowed the actual reaction temperature to be recorded. Another thermocouple placed on the wall of the furnace allowed to control the reactor temperature. The reactor outlet gases were analyzed by two gas chromatographs, one equipped with a thermal conductivity detector (TCD) (Shimadzu GC-8A) and the other equipped with a flame ionization detector (FID) (Carlo Erba Fractovap 2150 series). Using the FID-

Table 1 – Nomenclature and composition of the tested catalysts.

Catalyst	Pt (wt.%)	Co (wt.%)	Co/Pt (at/at)
1Pt	1	0	0
1.5Co	0	0.45	–
4Co	0	1.20	–
1Co1Pt	1	0.30	1
1.5Co1Pt	1	0.45	1.5
2Co1Pt	1	0.60	2
4Co1Pt	1	1.21	4

equipped chromatograph, the concentrations of CO and CO_2 were determined after separating them on a Porapak Q 60/80 mesh packed column (3 m length, 3 mm internal diameter). Once separated, CO and CO_2 were submitted to a methanation process at 450 °C, using an alumina-supported nickel catalyst and H_2 as carrier gas. The chromatograph with the TCD allowed quantifying O_2, H_2 and N_2. For each test, 50 mg of catalyst were used. After loading the reactor, N_2 was circulated in order to eliminate gases which might be adsorbed on the surface, especially O_2.

Before carrying out the CO selective oxidation reaction is essential to activate the catalyst. For this purpose, the catalyst sample was reduced under a H_2 flow of 60 cm^3/min, increasing the temperature from room temperature to 500 °C with a heating rate of 10 °C/min, and keeping the system for 20 min at the maximum temperature. Then, the catalyst was cooled to room temperature under the same hydrogen flow. Once this stage was finished, the reactants were admitted to the reactor. The reactor was fed with a gas mixture (total flow = 100 mL/min) having the following volumetric composition: O_2 = 0.49%, N_2 = 15.85%, CO = 0.97%, He = 8.71%, H_2 = 73.98%. The oxygen concentration is slightly higher than the stoichiometric value. Activity tests were performed from room temperature to *ca.* 300 °C.

Eqs (6)–(8) are used to calculate the CO conversion, the O_2 conversion and the selectivity to CO:

$$CO\ Conversion\ \% = \frac{[CO]_{in} - [CO]_{out}}{[CO]_{in}} \times 100 \quad (6)$$

$$O_2\ Conversion\ \% = \frac{[O_2]_{in} - [O_2]_{out}}{[O_2]_{in}} \times 100 \quad (7)$$

$$O_2\ Selectivity\ \% = 0.5 \times \frac{[CO]_{in} - [CO]_{out}}{[O_2]_{in}} \times 100 \quad (8)$$

where $[x]_{in}$ represents the inlet concentration of the x gas and $[x]_{out}$ represents the concentration of the same gas at the reactor outlet.

Stability test

With the aim of determining the stability of the catalysts, a test was conducted using the CoPt 1.5:1 catalyst. The reaction was started in the manner described in the previous section, but once the temperature reached a preset value (either 85 °C or 110 °C), it was kept constant at that value at least for 7 h.

Results and discussion

Catalyst characterization

The XRD spectra of the calcined support and of 4Co and 4Co1Pt catalysts were recorded, and are shown in Fig. 1. The diffraction patterns consisted mostly of broad peaks of poorly crystallized γ-Al_2O_3. Even though the samples with the highest Co loadings were analyzed, cobalt signals could not be detected. Also, no diffraction peaks were observed for Pt in the 4Co1Pt sample. These results suggest that Pt and Co particles

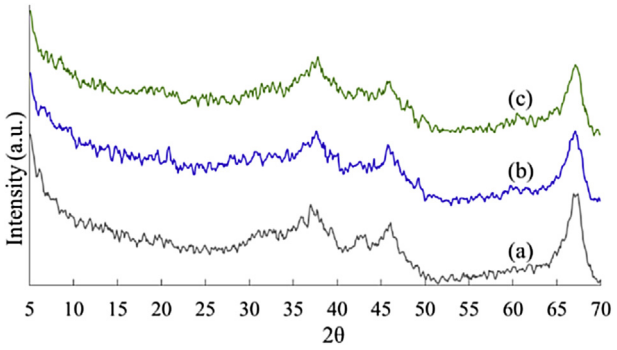

Fig. 1 – X-ray diffraction spectra of (a) γ-Al_2O_3 support and (b) 4Co and (c) 4Co1Pt catalysts.

are either amorphous or are too small to be detected by XRD methods. Similar results were found by other authors [4].

The patterns obtained in the TPR tests of catalysts are shown in Fig. 2. A common feature of the TPR corresponding to Pt-containing catalysts is that the existence of peaks assigned to the presence of chlorides, which are reduced at 400 °C [15], is discarded since these species were removed by chemical treatment during the preparation process of the monometallic catalyst. Regarding the cobalt-containing catalysts, the presence of hydrogen consumption peaks due to the existence of residual nitrates is also discarded, since the calcination carried out at 500 °C ensures the decomposition of nitrates, which takes place at *ca.* 300 °C [16].

Monometallic 1.5Co and 4Co catalysts presented a single reduction peak that is centered around 450°C-470 °C. This peak is usually assigned to the reduction of Co_3O_4 to CoO. When increasing the cobalt loading, the temperature of this reduction peak increases, revealing changes in the degree of interaction between the support and cobalt species. According to the literature, at temperatures around 600 °C, is possible to find another peak which corresponds to the reduction of different types of aluminates and CoO to metallic cobalt [17].

The TPR profile of the 1Pt catalyst showed two peaks: one centered at 185 °C and the other around 460 °C. The low temperature peak is assigned to the reduction of either PtO_2 or bulk PtOx species interacting with the oxygen atoms of the support. The presence of these species may be related to the

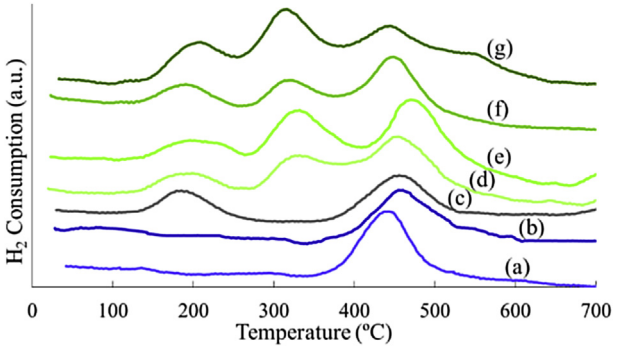

Fig. 2 – TPR profiles of the studied catalysts: (a) 1.5Co; (b) 4Co; (c) 1Pt; (d) 1Co1Pt; (e) 1.5Co1Pt; (f) 2Co1Pt and (g) 4Co1Pt.

ability of the alumina to stabilize oxidized Pt particles on its surface [18]. The second peak can be attributed to highly dispersed particles with strong interaction with the support [19,20].

The reduction profiles of all the bimetallic catalysts exhibited three peaks of hydrogen consumption. The first and the third peaks, assigned to the reduction of platinum species, are still observed at the same temperature as in the monometallic 1Pt catalyst. The second peak observed between the other two, around 350 °C, is assigned to the reduction of cobalt oxides in intimate interaction with platinum. This peak could be indicating the formation of a bimetallic Co-Pt phase. In addition, it is observed that increasing the cobalt loading, this central peak slightly shifts to lower temperatures, a fact that could be due either to the influence exerted by platinum, lowering the temperature at which cobalt species are reduced or to the decrease in the interaction of the metallic species with the support [21,22].

Fig. 3 shows the DR spectra in the UV–Vis region for the bimetallic PtCo studied catalysts. The spectra of two alumina-supported Co catalysts having two different concentration levels (1.5Co and 4Co), are also shown. The spectra of the Co samples calcined at 500 °C are characterized by two bands with maxima around 580 and 625 nm and a shoulder at 545 nm, characteristic of the presence of Co^{2+} ions in tetrahedral coordination, as found in the spinel structure $CoAl_2O_4$. The formation of spinel-type structures involve solid state reactions with Co^{2+} ions diffusion inwards the holes of the alumina and their distribution may vary with the cobalt content. The presence of $CoAl_2O_4$ species is undesirable because of the low reducibility that cobalt has in these species, generating catalysts with low activity [23].

When analyzing the DR spectra of the PtCo bimetallic catalysts (upper curves) two main features appear: i) the signals of tetrahedrally coordinated Co^{2+} ions (indicative of the interaction of Co with alumina as $CoAl_2O_4$) are no longer present and ii) a small band at 480 nm appears, that could be assigned to octahedral Co^{2+} ions. These are indicating that when Pt has been deposited on alumina before Co, the migration of Co^{2+} ions into the alumina lattice is inhibited, thus favoring the interaction between the two metals on the surface of the catalysts.

Fig. 4 and Table 2 shows the EXAFS fit results obtained at Pt L_3-edge. The Fourier transform corresponding to the monometallic Pt/Al_2O_3 sample, presents a main peak at 2.74 Å (without phase correction), corresponding to the Pt–Pt distance, indicating that the Pt atoms are mostly reduced. A small Pt-O contribution is observed at 2.00 Å, which can be associated to the interaction of Pt atoms with alumina. The Pt-Pt coordination number is lower than the corresponding to a platinum foil, due to the dispersion of the metallic phase.

Under the supposition of spherical particles, the average Pt-Pt coordination number obtained would correspond to 1.8 nm particles [24]. This particle size agrees well with the value found by TEM when measuring $Pt/\gamma\text{-}Al_2O_3$ catalysts prepared in our research group and reported previously elsewhere [25]. For the bimetallic catalysts, three coordination shells around Pt atoms are found: one of O atoms, one of Pt atoms and one of Co atoms; the last one indicates the formation of a CoPt alloy phase. In all bimetallic samples, the average coordination numbers of each metallic shell are very similar, showing that the proportion of alloy formed does not depend on the quantity of cobalt, at least for the studied atomic ratios. This can be explained taking into account the limited quantity of available Pt atoms to form the alloy phase. In the stoichiometric CoPt and Pt_3Co alloys, the ratios $N_{Pt\text{-}Pt}/N_{Pt\text{-}Co}$ are 0.5 and 2 respectively. The corresponding obtained ratio in our samples is about 2.5_3, consistently with the formation of the Pt_3Co alloy. In Pt_3Co, the Pt-Co and Pt-Pt distance is 2.71 Å, which is longer than the value fitted from our results with a difference of 0.09 Å at most. For particles in the nanometric scale it is expected that the distances can be contracted up to 0.1 Å [26–29] thus, being in these samples within the expected range.

The XANES results at the Co K-edge in the bimetallic catalysts (Fig. 5) shown that the cobalt is mainly in oxidized state,

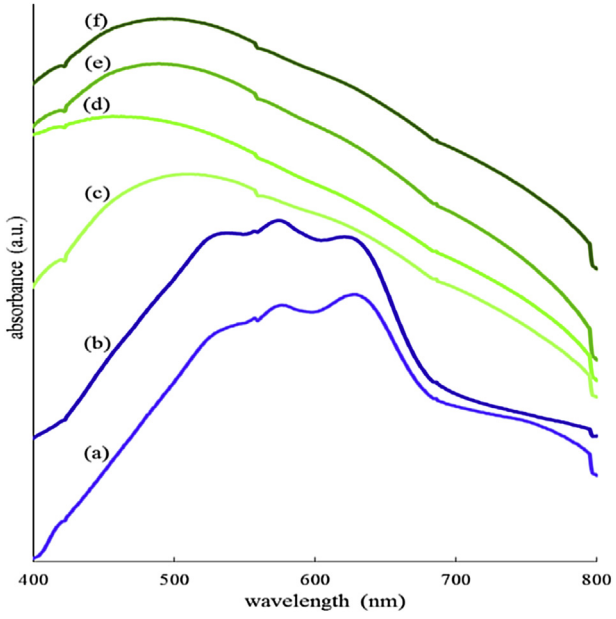

Fig. 3 – UV–VIS diffuse reflectance spectra of (a) 1.5Co; (b) 4Co; (c) 1Co1Pt; (d) 1.5Co1Pt; (e) 2Co1Pt and (f) 4Co1Pt samples.

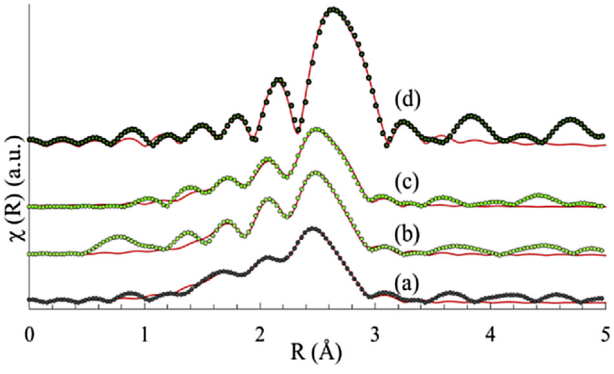

Fig. 4 – EXAFS fits of fresh catalysts in R-space at Pt L_3-edge: (a) 4Co1Pt; (b) 1.5Co1Pt; (c) 1Co1Pt; (d) 1Pt (symbols: experimental data, solid line: fits).

Table 2 – Structural parameters obtained from the EXAFS fits at the Pt L_3-edge.

Sample	Pt-O			Pt-Co			Pt-Pt		
	N	R(Å)	DWF(Å^2)	N	R(Å)	DWF(Å^2)	N	R(Å)	DWF(Å^2)
1Pt	0.4_2	2.00_1	0.012_4	–	–	–	8.6_6	2.753_3	0.0060_3
1Co1Pt	0.6_3	2.06_2	0.007_3	2.1_5	2.63_1	0.014_4	5.9_7	2.698_5	0.0080_6
1.5Co1Pt	0.8_3	2.05_2	0.010_3	2.4_5	2.62_1	0.012_3	5.4_7	2.687_4	0.0080_6
4Co1Pt	1.2_4	2.07_3	0.009_4	2.2_6	2.64_3	0.014_4	5.8_8	2.672_6	0.0090_7

N: Average coordination number. R: Interatomic distance. DWF: Debye–Waller factor.

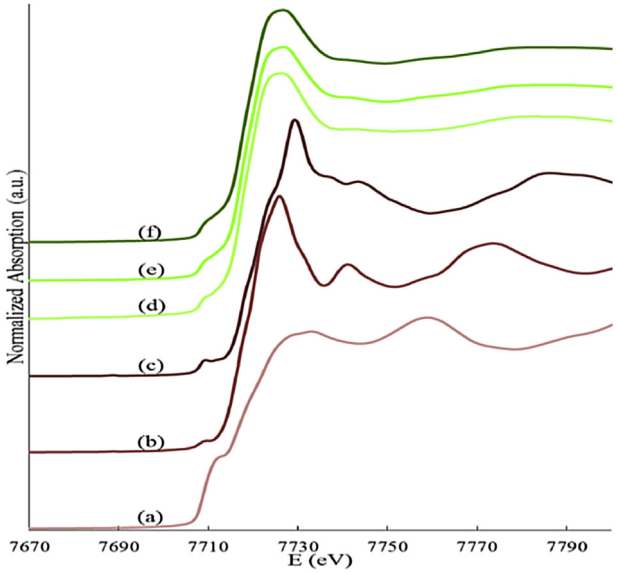

Fig. 5 – Normalized Co K-edge XANES spectra: (a) Co; (b) CoO; (c) Co_3O_4; (d) 1Co1Pt; (e) 1.5Co1Pt; (f) 4Co1Pt.

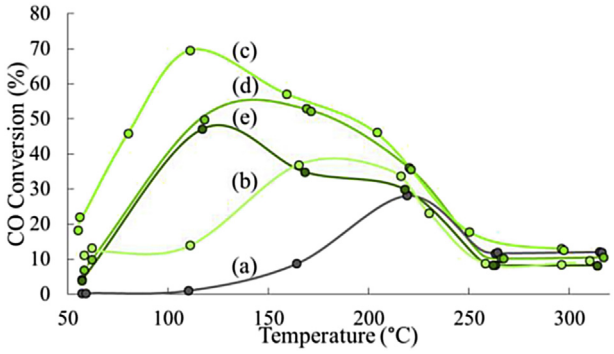

Fig. 6 – Variation of CO conversion as a function of the reaction temperature for the CO-PROX reaction over the studied catalysts (for reaction conditions, see the text): (a) 1Pt; (b) 1Co1Pt; (c) 1.5Co1Pt; (d) 2Co1Pt; (e) 4Co1Pt.

and the type of oxide formed is CoO, thus only a small fraction of atoms would be forming the alloy. As there is only a small fraction of Co atoms in metallic state, it would be not possible to form a CoPt alloy in the 1Co1Pt sample without have a significant amount of segregated metallic Pt, which should be reflected in the coordination number $N_{Pt\text{-}Pt}$. This reinforces the hypothesis that the alloy formed is the Pt_3Co one.

Based on these results, it is proposed that part of the Pt and Co atoms form bimetallic particles in which the cobalt electronic density decreases due to the electron transfer towards platinum. This is in good agreement with previously discussed TPR results, which also suggest the formation of bimetallic Pt–Co particles [4,30] In sum, it is proposed that on the surface of Pt–Co/Al_2O_3 catalysts there are clusters formed mainly by a Pt_3Co nano-alloy and CoO particles in intimate contact.

Catalytic activity

The results of the activity tests in the PROX reaction are shown in Fig. 6. This figure represents the conversion *vs.* reaction temperature for the tests of the PROX reaction carried out with a feed having a stoichiometric CO/O_2 ratio and excess H_2. At 50 °C, whatever the catalyst, the reaction reaches a conversion of 20% at the best. Then, there is a sharp rising for almost all the catalysts, with a maximum conversion for reaction temperatures between 100 and 150 °C.

The shape of the curve corresponding to the conversion of CO as a function of temperature on the 1Pt catalyst, agrees with that obtained in previous investigations [12]. Oxidation of CO on this catalyst is a multi-step process obeying a single-site competitive Langmuir–Hinshelwood mechanism, where CO, H_2 and O_2 compete for the noble metal surface. According to thermodynamics, CO is more strongly adsorbed on the noble metal than H_2 or O_2. Therefore at low temperature, CO is adsorbed on nearly the entire surface of the platinum preventing other species to do so. Then, it can be said that CO presents an inhibitory effect at low temperatures. With increasing temperature, up to about 115 °C, CO desorption starts, leaving free sites where O_2 and H_2 can adsorb. Thus, the reaction starts. A further increase in temperature produces more CO molecules to desorb, resulting in an increased conversion of the reactants.

When working at temperatures higher than 100 °C, the total O_2 consumption is observed for all catalysts. Due to this fact and taking into account that the feeding has a CO_2/O_2 stoichiometric ratio, selectivity and conversion values are equal at temperatures above 100 °C.

At 220 °C the maximum conversion and selectivity for the PROX reaction is reached. Beyond this temperature, the adsorption of H_2 becomes important and secondary reactions can take place: the reverse WGS and the oxidation of H_2 (Eqs. (1) and (3)), both leading to a decrease in CO conversion and selectivity. Additionally, at these temperatures, some traces of methane have also been detected.

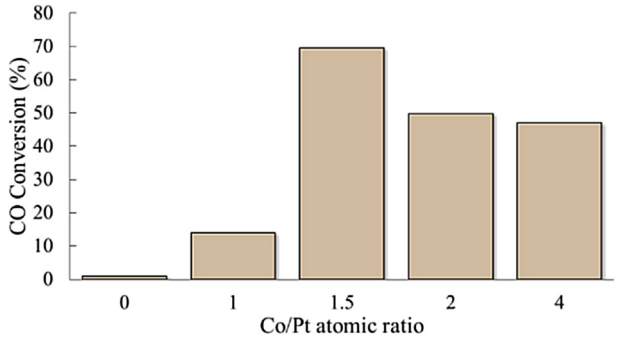

Fig. 7 – Effect of the Co/Pt atomic ratio on the CO conversion measured at 110 °C for the PROX reaction.

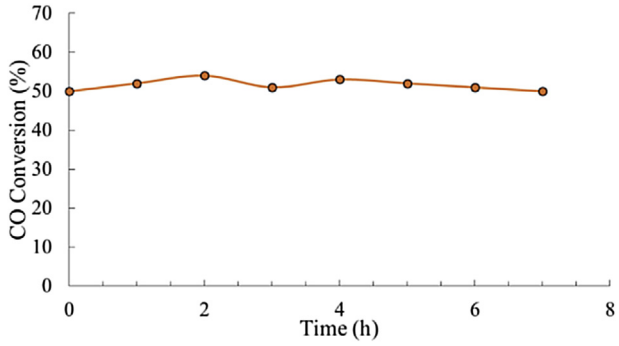

Fig. 8 – Stability performance of the 1.5Co1Pt catalysts for the PROX reaction at 85 °C.

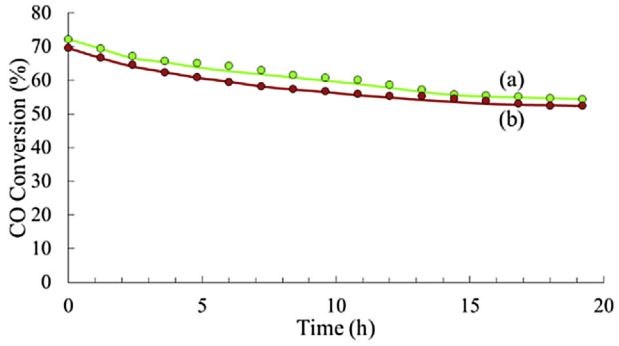

Fig. 9 – Stability performance of the 1.5Co1Pt catalysts for the PROX reaction at 110 °C: (a) Fresh; (b) Regenerated.

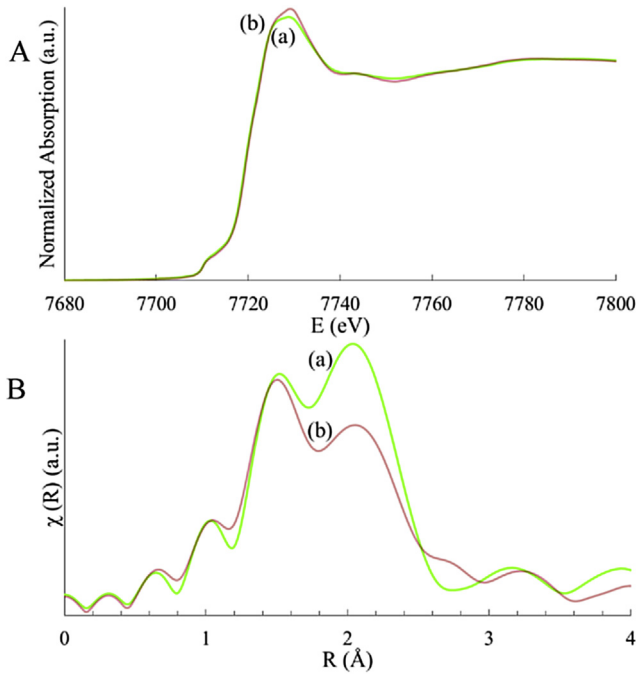

Fig. 10 – Normalized Co K-edge XANES spectra (A) and Fourier Transform (B) of fresh (a) and used (b) 1.5Co1Pt catalyst.

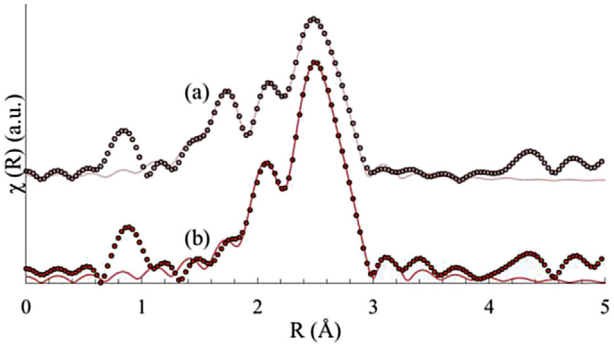

Fig. 11 – EXAFS fits of the used (a) and regenerated (b) 1.5Co1Pt catalyst in R-space at Pt L_3-edge (filled symbols: experimental data, solid line: fits).

For all the catalysts analyzed in this work it could be observed a beneficial effect of the addition of cobalt. When certain transition metal promoters, e.g. cobalt, are added to platinum catalysts, the kinetics of the PROX reaction is usually explained by a noncompetitive Langmuir–Hinshelwood mechanism with two types of active sites. The first type of active site is the promoter metal, Co. The promoter is in a low oxidation state and on that type of sites, O_2 is adsorbed and dissociates. Thus, Co activates oxygen. The second type of active sites is provided by Pt: as in the case of unpromoted catalyst, CO is adsorbed on it (although less strongly due the electronic modification of platinum) and then reacts with the dissociated oxygen atoms, leading to the selective oxidation of CO to give CO_2. The good or bad performance of a promoter depends on its ability to dissociate the molecular oxygen present in the gas phase and on the amount of active sites that provides for oxygen adsorption. A good promoter must easily change from one oxidation state to a different one, allowing the mobility of the oxygen vacancies [10]. Among the bimetallic catalysts studied in this paper, the best activity and selectivity corresponded to the 1.5Co1Pt catalyst.

To understand the decrease in the activity observed for all the catalysts at temperatures higher than 200 °C, it should be taken into account the presence of the aforementioned secondary reactions: the reaction between H_2-O_2 (which is not dominant at low temperature due to its high activation energy and the WGS reaction [7]).

In Fig. 7 the effect of cobalt concentration on the PROX reaction is observed. Taking into account the results of the

Table 3 – Results obtained from the EXAFS fits at the Pt L_3-edge of the used and regenerated 1.5Co1Pt catalyst.

Sample	Pt-O			Pt-Co			Pt-Pt		
1.5Co1Pt	N	R(Å)	DWF(Å^2)	N	R(Å)	DWF(Å^2)	N	R(Å)	DWF(Å^2)
Used	1.3_2	2.10_1	0.005_2	1.9_2	2.62_1	0.011_2	4.0_7	2.679_5	0.0067_6
Regenerated	0.5	2.10_6	0.008_3	2.3_2	2.62_3	0.011_2	5.4_8	2.688_6	0.0068_6

N: Average coordination number. R: Interatomic distance. DWF: Debye–Waller factor.

characterizations performed on the catalysts prepared, the behavior of the bimetallic catalysts could be explained as follows: when the Co/Pt ratio is lower than 1.5, the CO conversion is low due to the low concentration of the promoter and when the Co/Pt ratio is greater than 1.5, the high proportion of Co would be blocking a substantial number of active sites. Thus, a Co/Pt atomic ratio of 1.5 seems to correspond to a good balance between an electronically modified Pt (due to the presence of PtCo in intimate contact, according to TPR results) that adsorbs CO less strongly than in the absence of Co [10], and a suitable concentration of Co under the form of CoO (according to XANES results) that has the ability to dissociate the molecular oxygen.

Catalytic stability

The 1.5Co1Pt catalyst was submitted to a stability test at a constant temperature of 85 °C, and the results are displayed in Fig. 8. It is observed that the conversion of CO is almost constant throughout the 7 h of the test. At higher working temperatures, a certain catalytic deactivation appears (Fig. 9). CO oxidation studies indicate that the cobalt, which is forming a bimetallic Co-Pt phase, is oxidized as the reaction proceeds.

During the PROX reaction, this species provides an oxygen atom to the CO retrieving it from the O_2 of the gas phase. Then, one can infer that the loss in activity is due to changes in the stability of the cobalt oxides formed during the reaction. The oxides formed would have a higher stability, and therefore, would be less likely to participate in the selective oxidation of CO, with the consequent reduction of the activity with time.

This hypothesis was confirmed by XAS measurements of these samples at the Co K-edge. Fig. 10(A) show a small increment of the white line at the Co K edge of the catalyst 1.5Co1Pt after the reaction. This is an indication that more CoO is being form during the reaction. A similar result is observed in the Fourier transform of the EXAFS spectrum at the Co K edge (Fig 10B) where a decrease of the contribution from metallic phase is observed. These results confirm the hypothesis that the loose of activity is related to the changes in the stability of the CoO phase formed during the reaction.

Subsequent regeneration tests showed that the activity could be recovered after a reducing treatment performed at high temperature (500 °C). After that treatment, the catalyst recovered almost the same activity that had at the beginning of the reaction (see Fig. 9). Fig. 11 and Table 3 show the results of the EXAFS fits at the Pt L_3-edge in the samples used and regenerated. It is observed that, after regeneration, there is a decrease of the Pt-O fraction as well as an increment of the Pt-Co and Pt-Pt coordination numbers, showing an increase of the quantity of Pt atoms forming the alloy phase. The coordination numbers obtained for the catalyst after regeneration are very similar to those obtained before the reaction confirming that the recovery of the activity is related to the proportion of metallic phases present in the catalyst.

Conclusions

By adding cobalt to a Pt/γ-Al_2O_3 catalyst, a significant improvement in CO conversion in the PROX reaction is obtained. This improvement could be assigned to the existence of a strong interaction between cobalt and platinum, decreasing in this way the Pt-support interaction. Most likely a new Pt-Co phase with lower reduction temperature and high synergy is formed. The catalytic performance reaches its maximum value for a Co/Pt atomic ratio of 1.5. The addition of Co above this value causes a decrease in activity, since it would result in a covering of the Pt active sites, preventing the adsorption of CO.

All the bimetallic catalysts studied showed the maximum conversion in the range 110–180 °C. This value is within the range of acceptable temperatures for this process. A further increase in temperature causes a decrease in the conversion of CO, either because at such temperatures begin to be noticeable the reverse WGSR or because the adsorption of CO is not so strong, and the active sites that are released can be occupied by H_2, which reacts to form water.

The catalyst with the best activity, 1.5Co1Pt, did not show a significant deactivation after several hours of operation at 85 °C. At higher working temperatures, the deactivation was more pronounced, but the original activity was almost recovered when submitting the catalysts to a reduction process at 500 °C. This fact indicates that there is no sintering of the metallic phase in the course of the reaction and that the deactivation is due to the oxidation of cobalt.

Acknowledgements

This work was supported by Consejo Nacional de Investigaciones Científicas y Técnicas (CONICET) (PIP 0276 and PIP 1035), Universidad Nacional de La Plata (Projects X700 and I152) and Laboratório Nacional de Luz Síncrotron (LNLS, Brasil) (Project XAFS1-18859).

REFERENCES

[1] Zhao Z, Yung M, Ozkan U. Effect of support on the preferential oxidation of CO over cobalt catalysts. Catal Commun 2008;9:1465–71.

[2] Iulianelli A, Ribeirinha P, Mendes A, Basile A. Methanol steam reforming for hydrogen generation via conventional and membrane reactors: A review. Renew Sustain Energy Rev 2014;29:355–68.
[3] Bion N, Epron F, Moreno M, Mariño F, Duprez D. Preferential oxidation of carbon monoxide in the presence of hydrogen (PROX) over noble metals and transition metal oxides: advantages and drawbacks. Top Catal 2008;51:76–88.
[4] Li H, Yu X, Tu S, Yan J, Wang Z. Catalytic performance and characterization of Al_2O_3-supported Pt–Co catalyst coatings for preferential CO oxidation in a micro-reactor. Appl Catal A Gen 2010;387:215–23.
[5] Kwak C, Park T, Suh D. Preferential oxidation of carbon monoxide in hydrogen-rich gas over platinum–cobalt–alumina aerogel catalysts. Chem Eng Sci 2005;60:1211–7.
[6] Callaghan CA. Kinetics and catalysis of the water-gas-shift reaction: a microkinetic and graph theoretic approach. Thesis. 2006.
[7] Woods M, Gawade P, Tan B, Ozkan U. Preferential oxidation of carbon monoxide on Co/CeO_2 nanoparticles. Appl Catal B Environ 2010;97:28–35.
[8] Uğuz K, Yildirim R. Comparative study of selective CO oxidation over Pt-Co-M/Al_2O_3 catalysts (M=Ce, Mg, Mn, Zr, Fe) in hydrogen-rich streams: effects of a second promoter. Turk J Chem 2009;33:545–53.
[9] Brown M, Green B. Treatment of gases, U.S. Patent 3088919 1963.
[10] Jain SK, Crabb EM, Thompsett D, Steele AM. Controlled modification of Pt/Al_2O_3 for the preferential oxidation of CO in hydrogen: A comparative study of modifying element. Appl Catal B Environ 2009;89:349–55.
[11] Bideberripe HP, Ramallo-López JM, Figueroa SJA, Jaworski MA, Casella ML, Siri GJ. Ge-modified Pt/SiO_2 catalysts used in preferential CO oxidation (CO-PROX). Catal Commun 2011;12:1280–5.
[12] Siri GJ, Bertolini GR, Ferretti OA. Preferential oxidation of Co in presence of H_2 behavior of PtSn/γ-Al_2O_3 catalysts modified by K or Ba. Lat Am Appl Res 2007;37:275–81.
[13] Ravel B, Newville MJ. ATHENA, ARTEMIS, HEPHAESTUS: data analysis for X-ray absorption spectroscopy using IFEFFIT. Synchrotron Radiat 2005;12:537–41.
[14] Zabinsky SI, Rehr JJ, Ankudinov A, Albers RC, Eller MJ. Multiple-scattering calculations of x-ray-absorption spectra. Phys Rev B 1995;52:2995–3009.
[15] Navarro RM, Álvarez-Galván MC, Cruz Sánchez-Sánchez M, Rosa F, Fierro JLG. Production of hydrogen by oxidative reforming of ethanol over Pt catalysts supported on Al_2O_3 modified with Ce and La. Appl Catal B Environ 2005;55:229–41.
[16] Enache DI, Roy-Auberger M, Revel R. Differences in the characteristics and catalytic properties of cobalt-based Fischer–Tropsch catalysts supported on zirconia and alumina. Appl Catal A Gen 2004;268:51–60.
[17] Backman LB, Rautiainen A, Lindblad M, Krause AOI. The interaction of cobalt species with alumina on Co/Al_2O_3 catalysts prepared by atomic layer deposition. Appl Catal A Gen 2009;360:183–91.
[18] El Doukkali M, Iriondo A, Jalowiecki-Duhamel L, Dumeignil F. A comparison of sol–gel and impregnated Pt or/and Ni based γ-alumina catalysts for bioglycerol aqueous phase reforming. Appl Catal B Environ 2012;125:516–29.
[19] Zanuttini MS, Lago CD, Querini CA, Peralta MA. Deoxygenation of m-cresol on Pt/γ-Al_2O_3 catalysts. Catal Today 2013;213:9–17.
[20] Meephoka C, Chaisuk C, Samparnpiboon P, Praserthdam P. Effect of phase composition between nano γ- and χ-Al_2O_3 on Pt/Al_2O_3 catalyst in CO oxidation. Catal Commun 2008;9:546–50.
[21] Suh DJ, Kwak C, Kwon SM, Park TJ. Removal of carbon monoxide from hydrogen-rich fuels by selective low-temperature oxidation over base metal added platinum catalysts. J Power Sources 2005;142:70–4.
[22] Jacobs G, Das TK, Racoillet G, Davis BH. Fischer–Tropsch synthesis: support, loading, and promoter effects on the reducibility of cobalt catalysts. Appl Catal A Gen 2002;233:263–81.
[23] Liotta LF, Pantaleo G, Macaluso A, Di Carlo G, Deganello G. CoO_x catalysts supported on alumina and alumina-baria: influence of the support on the cobalt species and their activity in NO reduction by C_3H_6 in lean conditions. Appl Catal A Gen 2003;245:167–77.
[24] Ramallo-López JM, Requejo FG, Craievich AF, Wei J, Avalos-Borja M, Iglesia E. Complementary methods for cluster size distribution measurements: supported platinum nanoclusters in methane reforming catalysts. J Mol Catal A Chem 2005;228:299–307.
[25] Jaworski MA, Vetere V, Bideberripe HP, Siri GJ, Casella ML. Structural aspects of PtSn/γ-Al_2O_3 catalysts prepared through surface-controlled reactions: behavior in the water denitrification reaction. Appl Catal A Gen 2013;453:227–34.
[26] Wijnen PWJG, Van Zon FBM, Koningsberger DC. Determination of metal particle size in partly reduced Ni catalysts by hydrogen/oxygen chemisorption and EXAFS. J Catal 1988;114:463–8.
[27] Kang JH, Menard LD, Nuzzo RG, Frenkel AI. Unusual non-bulk properties in nanoscale materials: thermal metal–metal bond contraction of γ-alumina-supported Pt catalysts. J Am Chem Soc 2006;128:12068–9.
[28] Bus E, Miller JT, Kropf AJ, Prins R, van Bokhoven JA. Analysis of in situ EXAFS data of supported metal catalysts using the third and fourth cumulant. Phys Chem Chem Phys 2006;8:3248–58.
[29] Lei Y, Jelic J, Nitsche L, Meyer R, Miller J. Effect of particle size and adsorbates on the L3, L2 and L1 X-ray absorption near edge structure of supported Pt nanoparticles. Top Catal 2011;54:334–48.
[30] Zheng R, Porosoff MD, Weiner JL, Lu S, Zhu Y, Chen JG. Controlling hydrogenation of CO and CC bonds in cinnamaldehyde using silica supported Co-Pt and Cu-Pt bimetallic catalysts. Appl Catal A Gen 2012;419–420:126–32.